ChemComm

COMMUNICATION

The synergy between the $CsPbBr_3$ nanoparticle surface and the organic ligand becomes manifest in a demanding carbon–carbon coupling reaction†

Cite this: DOI: 10.1039/d0cc01339k

Received 20th February 2020,
Accepted 25th March 2020

DOI: 10.1039/d0cc01339k

rsc.li/chemcomm

Ignacio Rosa-Pardo,[a] Carla Casadevall,[b] Luciana Schmidt,[a] Miguel Claros,[b] Raquel E. Galian,*[a] Julio Lloret-Fillol*[bc] and Julia Pérez-Prieto*[a]

We demonstrate here the suitability of $CsPbBr_3$ nanoparticles as photosensitizers for a demanding photoredox catalytic homo- and cross-coupling of alkyl bromides at room temperature by merely using visible light and an electron donor, thanks to the cooperative action between the nanoparticle surface and organic capping.

Lead halide perovskites with the formula $APbX_3$, where A is a small-sized monocation (such as $CH_3NH_3^+$, Cs^+) and X is a halide anion (Cl^- Br^-, I^-), present a three-dimensional inorganic framework consisting of corner-sharing PbX_6 octahedra and small-sized cations in the voids between them (Fig. S1, ESI†). These are promising semiconductors for low-cost solar energy conversion, due to their effectiveness in charge separation as well as hole and electron transport.[1–4] These qualities are also essential for their application in photocatalysis, since the photogenerated charges are trapped at different surface sites and concerted interfacial electron transfer reactions with electron acceptor and electron donor substrates can occur if their reduction potentials are within the bandgap. The performance of $APbX_3$ in photovoltaics has proved to be superior to that of II–VI semiconductors,[5] and this can also apply to light-induced catalytic organic transformations.[6–10]

$APbX_3$ perovskite nanocrystals (NCs) share some similarities with CdSe and CdTe quantum dots, in particular, a strong absorption and a wide spectrum extending well into the Vis range, a narrow emission peak and electronic properties tuneable with the composition and size of the NCs.[11–15] However, contrary to them and due to their defect tolerance, core $APbX_3$ perovskite NCs can be synthesized with a photoluminescence quantum yield (QY_{PL}) of up to 100%[16–18] without the need of any electronic passivation with an inorganic material that has a wider bandgap. The tolerance of $APbX_3$ perovskites is attributed to the formation of defect states near the band edges.[19–21] Moreover, they can present considerable luminescence as bare nanoparticles.[22] On the contrary, in common semiconductors, the intrinsic defects are deeply located in the middle of the gap and, consequently, they can trap the carriers generated after excitation of the NCs, reducing the QY_{PL}.[23] In terms of photosensitized reactions, $APbX_3$ NCs have a higher conduction band (CB) edge, but also a higher valence band edge[24–26] therefore, $APbX_3$ NCs can be more effective photosensitizers for reduction of organic substrates, while CdS, CdSe and TiO_2[27–30] can be more effective for oxidation of organic substrates.[31–35] Y. Yan *et al.* have recently reported on the potential of the $CsPbBr_3$ NCs as photosensitizers for reductive C_{sp^3}–C_{sp^3} formation,[6,7] demonstrating the capacity of these perovskites to promote α-alkylation of aldehydes with α-bromoacetophenones. This process requires the presence of an organic co-catalyst (bis(2-chloroethyl)amine hydrochloride) and a base (2,6-lutidine). The C–C homocoupling of the acetophenone was selectively achieved by using (5*S*)-(−)-2,2,3-trimethyl-5-benzyl-4-imidazolidinone as the co-catalyst.[7]

Taking into account the CB edge energy of $CsPbBr_3$ and the redox potential of α-bromoacetophenone of about −0.96 V[11] and −0.25 V (*vs.* SHE),[36,37] respectively, the photoreduction of α-bromoacetophenone is thermodynamically exergonic, due to the fact that the excited state of the perovskite is a potent reductant and would enable the heterolytic cleavage of the C–Br bond.

A more demanding process is that of the photoredox α-benzylation of aldehydes with a less activated C–Br bond, such as that of benzyl bromide with a reduction potential, $E_{1/2}$, of −1.61 V *vs.* SHE in CH_3CN.[38] In fact, the strong reductant $Ir(ppy)_3$ excited state, $*Ir(ppy)_3$, ($E_{1/2}$ of −1.49 V *vs.* SHE in CH_3CN) fails to promote this process.[39]

These results motivated our study of the reductive C–C coupling of benzyl bromides by using $CsPbBr_3$ NCs as the photocatalyst and a tertiary amine as the electron donor (ED), bearing in mind that

[a] *Institute of Molecular Science (ICMol), University of Valencia c/Catedrático José Beltrán 2, Paterna, E46980 Valencia, Spain*
[b] *Institute of Chemical Research of Catalonia (ICIQ), The Barcelona Institute of Science and Technology, Avinguda Països Catalans 16, 43007 Tarragona, Spain*
[c] *Catalan Institution for Research and Advanced Studies (ICREA) Passeig Lluïs Companys, 23, 08010, Barcelona, Spain*

† Electronic supplementary information (ESI) available: Further spectra, characterization and data analysis. See DOI: 10.1039/d0cc01339k

the encapsulating effect of a NC lipophilic organic capping could approach the substrate and the ED to the perovskite surface, thus assisting the process and improving the photocatalysis.

Here is reported for the first time that the combination of visible light irradiation, DIPEA (*N,N*-diisopropylethylamine), and colloidal $CsPbBr_3$ enables the photocatalytic single-electron transfer to benzyl bromides, eventually leading to the benzyl radical and finally to the C–C homocoupling products. Turnover numbers (TON, moles of substrate transformed/moles of $CsPbBr_3$ NCs) higher than 17 500 were obtained. The formation of cross-coupling products was also tested by using two different benzyl bromides in the reaction.

First, colloidal $CsPbBr_3$ capped with dodecylamine (DDA) was prepared by the ligand assisted reprecipitation technique with some modifications (Fig. S1, ESI†).[40] The colloid concentration was estimated as 3.6 μM by using the molar coefficient reported for $CsPbBr_3$ nanocubes of 11 nm ($\varepsilon = 3.5 \times 10^6$ M^{-1} cm^{-1} at $\lambda = 510$ nm).[41] This material presented a major absorption peak at 500 nm and PL maximum at 510 nm in toluene (full width at half maximum, FWHM, of 20 nm, Fig. S2, ESI†), average PL lifetime (τ_{av}) of 34 ns and QY_{PL} of 31%.[40]

The $CsPbBr_3$ colloid was first evaluated as photocatalyst for the coupling of benzyl bromide **1a** to yield **1b**, using an in-house developed 48-well parallel photoreactor with the capacity to control the temperature and the radiation of the reactions (Fig. S3, bottom, ESI†). Two solvents of different polarity (toluene and ethyl acetate) and three EDs (trimethylamine, TEA; tri-phenylphosphine, PPh_3; DIPEA in 20, 10 and 3 equiv.) were tested. The mixture containing the perovskite (1.44 μM), **1a** (34 mM) and the ED was irradiated with Vis light (LED 447 ± 20 nm) at 30 °C for 20 h under nitrogen while soft stirred using a shaker (see details in ESI†). Screening of reaction conditions was first carried out; the yields were calculated by Gas Chromatography-Flame Ionization detector (GC-FID) analysis of the reaction crude using biphenyl as internal standard (see Table S1 in ESI† for further details). DIPEA was the best ED of the tested ones. In the case of using TEA and PPh_3, the formation of some white precipitate was seen with the naked eye. This is consistent with the formation of the corresponding quaternary salts (see Fig. S4, ESI†), whose precipitation may partly justify their lower efficacy as ED. Therefore, DIPEA was selected as the ED for the rest of the study. Table 1 shows the results of the photocatalyzed homo- and cross-coupling of benzyl bromides in toluene; the values reported are GC-FID yields and/or isolated yields. Results in parenthesis represent isolated yields from 3 reactions irradiated at 447 nm (LED 1 W) for 60 h at 30 °C using an in-house developed 25-well parallel photoreactor (Fig. S3, top, ESI†).[42] In general, the chromatogram and ^{1}H-NMR spectrum analysed after the reaction were clean, showing only unreacted starting material, coupling products and internal standard (see Fig. S5–S13, ESI†). The mass loss could be attributed to the formation of the dehalogenation product, which for **1a** is toluene.

Formation of the homocoupling product **1b** was successful; the yield decreased slightly when using 10 instead of 20 equiv. of DIPEA. The the product yield depended on the nature of the *p*-substituent of the benzyl bromide and decreased in the following order: H, ^{t}Bu, OMe > Cl > Br. Considering the concentration of NCs in solution, TON up to 17 500 was estimated, illustrating these NCs are self-sufficient, in the sense that they do not require a co-catalyst, and are highly active to engage the demanding catalytic transformations (see below).

Table 1 Homo- and cross-coupling of benzyl bromides photocatalyzed by colloidal $CsPbBr_3$ perovskite[a]

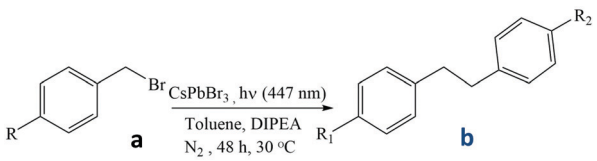

Run	Substrate	Product and Yield (%)[II, III] Blue $R_1 = R_2$ Green $R_1 \neq R_2$	
1	**1a** R = H	**1b** $R_{1,2}$ = H	83 (62)
2[IV]	**1a** R = H	**1b** $R_{1,2}$ = H	80
3[V]	**1a** R = H	**1b** $R_{1,2}$ = H	42
4	**2a** R = Br	**2b** $R_{1,2}$ = Br	52
5	**3a** R = OMe	**3b** $R_{1,2}$ = Me	75
6	**4a** R = Cl	**4b** $R_{1,2}$ = Cl	65 (60)
7	**5a** R = ^{t}Bu	**5b** $R_{1,2}$ = ^{t}Bu	79
8	**1a + 2a**	**1b** (18) **6b**[VI] (51)	**2b** (30)
9	**1a + 3a**	**1b** (28) **7b**[VI] (39)	**3b** (32)
10	**2a + 3a**	**2b** 22 **8b**[VI] (44)	**3b** (27)

[a] General conditions of the reaction: $CsPbBr_3$ (1.44 μM), total substrate (34 mM; 17 mM of each substrate in the cross-coupling assays), 20 equiv. of DIPEA, solvent (toluene, total volume: 1 mL), irradiation at 447 ± 20 nm during 48 h at 30 °C under N_2, conversion 100%. [b] The results are average of at least 2 duplicates. [c] The values reported are GC-FID/^{1}H-NMR yields. Results in parenthesis represent isolated yields from 3 reactions at 30 °C irradiated for 60 h. [d] DIPEA (10 equiv.). [e] Two hours soft stirring in the shaker prior irradiation. [f] Cross-coupling obtained from run 8–10.

The reduction of the benzyl bromides used in this study was registered in toluene/CH_3CN (85 : 15, v : v) and they proved to be irreversible (see Fig. S14–S19, ESI†), with an onset potential at −1.50 V *vs.* SHE. DFT calculations for the one-electron reduction of benzyl bromide were in agreement with a found redox potential of −1.44 *vs.* SHE (see computational studies and Fig. S20 in ESI†). These values are significantly lower than the $CsPbBr_3$ redox potential considering the CB edge energy (−0.96 V *vs.* SHE), and therefore the formation of the benzyl radical is thermodynamically disfavoured. This is also true for the rest of the benzyl bromide series.

Then, we studied electronic effects by evaluating the reaction between different *p*-substituted benzyl bromides using the optimized conditions: $CsPbBr_3$ (1.44 μM), DIPEA (20 equiv.), toluene as solvent, irradiation at 447 nm of the as-prepared mixture at 30 °C for 48 h under nitrogen. Remarkably, homocoupling product **2b** was produced selectively *vs.* **1b** (run 8, Table 1), and there was some selectivity in the production of products **1b** and **3b** *vs.* the cross-coupling product **7** (run 9, Table 1). A nearly statistical mixture of products was obtained in the reaction of **2a** and **3a** (run 10, Table 1).

The small selectivity in the cross-coupling products observed for all cases together with the thermodynamically disfavoured formation of the benzyl radical intermediate is puzzling. However, it could be rationalized by substrate pre-concentration and, consequently, a high concentration of the generated radical anions in the nanoparticle surface (see discussion in ESI,† Section 6), favoured by the van der Waals interactions between the alkyl chains of the capping groups and the substrates.

Therefore, a very high substrate concentration could build enough benzyl bromide radical to facilitate the exergonic C–C bond formation driving the reaction forward but at expenses of selectivity (Fig. 1). Control experiments without either perovskite NCs or light, under otherwise same conditions, corroborated that C–C products did not form for any of the substrates included in Table 1 (experiments performed at least twice, Table S1, ESI†).

To gain some insight into the mechanism, we monitored the UV-Vis spectrum of a solution containing $CsPbBr_3$ under different conditions. First, a fresh solution of the perovskite in toluene while irradiating with the LED showed the appearance of two negative bands at 450 nm and at 510 nm assigned to scattered radiation and emission of the perovskite, respectively (Fig. S21, ESI†). The addition of benzyl bromide to this solution under irradiation did not change significantly the spectrum, thus suggesting that the excited state of the perovskite cannot directly activate the benzyl bromide. Accordingly, blank experiments showed the recovery of the benzyl bromide after irradiation. However, the addition of the ED to this solution led to a partial reduction of the emission of the band at 510 nm after 200 s (Fig. S22, ESI†). Interestingly, the reduction of the emission of the band at 510 nm is practically quantitative if the ED is added to a fresh $CsPbBr_3$ solution in the absence of the benzyl bromide (Fig. S23, ESI†). All together suggested that the $CsPbBr_3$ perovskite is reductively quenched by the ED and the reductive state of the perovskite was able to reduce the benzyl bromide to give the benzylic radical.

The HOMO energy level of trialkyl amines is reported at −5.76 eV,[43] *i.e.*, it is more positive than that of the perovskite valence band maximum (between −5.85 eV and −6.4 eV).[11,44] Consequently, there is a driving force for the hole transfer (between ∼0.1 and 0.6 eV) and, therefore, for the charge separation. In principle, generation of the benzyl bromide anion radical is not thermodynamically favourable, but the interaction between the benzyl bromide, preconcentrated within the organic capping, and with the NC surface[45,46,47] would facilitate the electron transfer process, eventually leading to the coupling products (Fig. 1). The recyclability of the perovskite was also tested using **1a** as the substrate. After the first catalytic run reported in Table 1, the perovskite was recovered by centrifugation and washed with toluene to remove unreacted organic substrate and formed products. The recovered perovskite was used in a second run again adding DIPEA (20 equiv.), the substrate and toluene, and irradiating for 20 h. The yield of **1b** significantly dropped to 3%. Further irradiation up to 60 h only produced an increase to 9%. The absorption spectrum of the sample showed a considerable increase of the scattering and the appearance of an excitonic peak at about 523 nm (compare Fig. S24a and b). The emission peak of the perovskite shifted from 517 nm to 523 nm and the emission efficiency, as well as the emission lifetime, decreased (QY_{PL} 14% and τ_{av} 21 ns). The addition of DDA (up to 70 μL from a stock solution of 5 mg mL^{-1}) to this sample led to (i) a decrease in the sample scattering and a blue shift of the excitonic peak to 515 nm and (ii) a high recovery of the perovskite emission and a peak shift to 519 nm (Fig. S24 c, ESI†). Moreover, transmission electron microscopy (TEM) images of the recovered perovskite showed it consisted of microsized perovskites together with an increase of perovskite NCs number (Fig. S24 d, ESI†). Note that the yield of the coupling product decreased significantly when the reaction mixture was softly stirred in the shaker for two hours before irradiation, (run 3, Table 1); this is consisting with

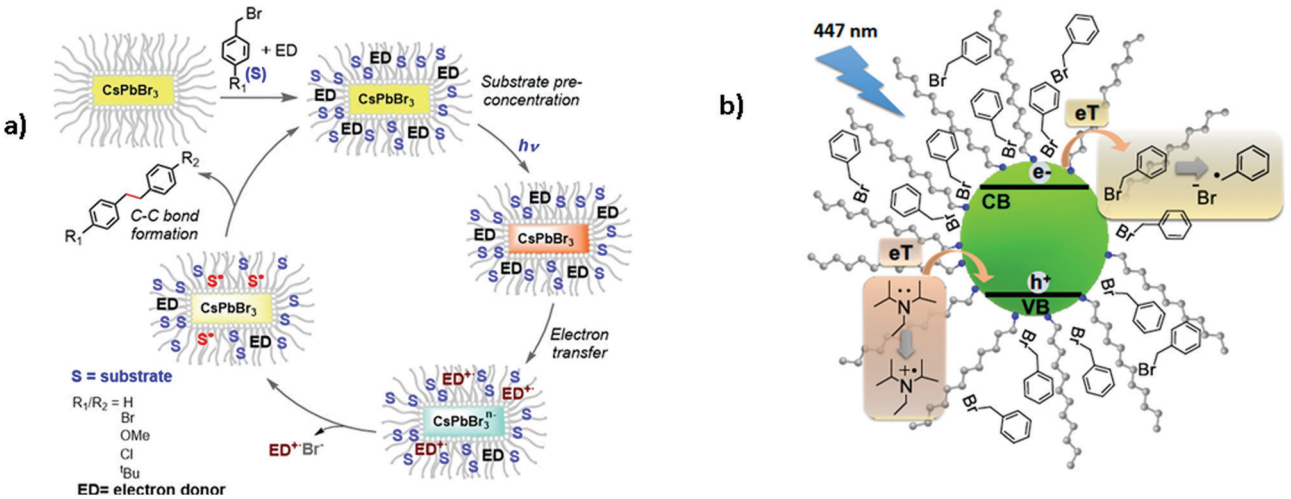

Fig. 1 Schematic representation of (a) the cooperative action between the NC surface and the capping for the catalysed coupling reaction and (b) of the processes occurring after Vis-excitation of the $CsPbBr_3$ in the presence of the benzyl halide (electron acceptor) and DIPEA (electron donor) encapsulated within the capping.

ligand removal from the NC surface by DIPEA. To determine if the low performance of the isolated perovskite was due to the removal of the ligands at the NC surface due to the washing treatment, the reaction was repeated under the same conditions and then, without work-up, we added again substrate (1 equiv.) and the mixture was shaken for additional 20 h under the otherwise same conditions. This experiment was repeated twice; the conversion of **1a** was about 66% and **1b** was obtained in a 45% yield (average values of two duplicates).

To sum up, for the first time it is demonstrated that colloidal $CsPbBr_3$ perovskite NCs are suitable as photosensitizers for photoredox catalytic homo-/cross-coupling of benzyl bromides at room temperature with TON up to 17 500 by merely using Vis light and an electron donor, such as DIPEA. This is a clear example of the potentiality of these perovskites in light-induced catalytic transformations, where the synergy between the ligand and the NC surface plays a crucial role. These results broaden the applicability of these materials in photocatalysis.

Thanks to MINECO (CTQ2017-82711-P, CTQ2016-80038-R, FPU17/05564 (I. R.-P.), FPU14/02550 (C. C.), partially co-financed with FEDER funds), GV (PROMETEO/2019/080 and IDIFEDER/2018/064), ICIQ Foundation, ERF for project FP7-PEOPLE-2010-ERG-268445 (J. L.-F.), and CELLEX Foundation (CELLEX-ICIQ high-throughput platform) and Dr F. Ungeheuer for his help in the photocatalytic reactions.

Conflicts of interest

Q4

Notes and references

1 A. Kojima, K. Teshima, Y. Shirai and T. Miyasaka, *J. Am. Chem. Soc.*, 2009, **131**, 6050–6051.
2 A. K. Jena, A. Kulkarni and T. Miyasaka, *Chem. Rev.*, 2019, **119**, 3036–3103.
3 H.-S. Kim, C.-R. Lee, J.-H. Im, K.-B. Lee, T. Moehl, A. Marchioro, S.-J. Moon, R. Humphry-Baker, J.-H. Yum and J. E. Moser, *Sci. Rep.*, 2012, **2**, 591.
4 M. M. Lee, J. Teuscher, T. Miyasaka, T. N. Murakami and H. J. Snaith, *Science*, 2012, **338**, 643–647.
5 Best Research-Cell Efficiency Chart, https://www.nrel.gov/pv/cell-efficiency.html, 2019.
6 X. Zhu, Y. Lin, J. San Martin, Y. Sun, D. Zhu and Y. Yan, *Nat. Commun.*, 2019, **10**, 2843.
7 X. Zhu, Y. Lin, Y. Sun, M. C. Beard and Y. Yan, *J. Am. Chem. Soc.*, 2019, **141**, 733–738.
8 J. A. Caputo, L. C. Frenette, N. Zhao, K. L. Sowers, T. D. Krauss and D. J. Weix, *J. Am. Chem. Soc.*, 2017, **139**, 4250–4253.
9 C. Huang, X.-B. Li, C.-H. Tung and L.-Z. Wu, *Chem. – Eur. J.*, 2018, **24**, 11530–11534.
10 A. K. Simlandy, B. Bhattacharyya, A. Pandey and S. Mukherjee, *ACS Catal.*, 2018, **8**, 5206–5211.
11 V. K. Ravi, G. B. Markad and A. Nag, *ACS Energy Lett.*, 2016, **1**, 665–671.
12 S.-Y. Joo, D.-W. Jeong, C.-G. Lee, B.-S. Kim, H.-S. Park and W.-B. Kim, *J. Appl. Phys.*, 2017, **121**, 223102.
13 H. Yu, H. Wang, J. Zhang, J. Lu, Z. Yuan, W. Xu, L. Hultman, A. A. Bakulin, R. H. Friend, J. Wang, X.-K. Liu and F. Gao, *Small*, 2019, **15**, 1804947.
14 L. Peng, A. Tang, C. Yang and F. Teng, *J. Alloys Compd.*, 2016, **687**, 506–513.
15 S. Gonzalez-Carrero, R. E. Galian and J. Pérez-Prieto, *Opt. Express*, 2016, **24**, A285–A301.
16 S. Gonzalez-Carrero, L. Francés-Soriano, M. González-Béjar, S. Agouram, R. E. Galian and J. Pérez-Prieto, *Small*, 2016, **12**, 5245–5250.
17 S. González-Carrero, L. Martínez-Sarti, M. Sessolo, R. E. Galian and J. Pérez-Prieto, *J. Mater. Chem. C*, 2018, **6**, 6771–6777.
18 F. Zhang, H. Zhong, C. Chen, X.-G. Wu, X. Hu, H. Huang, J. Han, B. Zou and Y. Dong, *ACS Nano*, 2015, **9**, 4533–4542.
19 V. S. Chirvony, S. González-Carrero, I. Suárez, R. E. Galian, M. Sessolo, H. J. Bolink, J. P. Martínez-Pastor and J. Pérez-Prieto, *J. Phys. Chem. C*, 2017, **121**, 13381–13390.
20 D. Meggiolaro, S. G. Motti, E. Mosconi, A. J. Barker, J. Ball, C. Andrea Riccardo Perini, F. Deschler, A. Petrozza and F. De Angelis, *Energy Environ. Sci.*, 2018, **11**, 702–713.
21 V. Adinolfi, M. Yuan, R. Comin, E. S. Thibau, D. Shi, M. I. Saidaminov, P. Kanjanaboos, D. Kopilovic, S. Hoogland, Z.-H. Lu, O. M. Bakr and E. H. Sargent, *Adv. Mater.*, 2016, **28**, 3406–3410.
22 S. Gonzalez-Carrero, L. C. Schmidt, I. Rosa-Pardo, L. Martínez-Sarti, M. Sessolo, R. E. Galian and J. Pérez-Prieto, *ACS Omega*, 2018, **3**, 1298–1303.
23 R. E. Brandt, J. R. Poindexter, P. Gorai, R. C. Kurchin, R. L. Z. Hoye, L. Nienhaus, M. W. B. Wilson, J. A. Polizzotti, R. Sereika, R. Žaltauskas, L. C. Lee, J. L. MacManus-Driscoll, M. Bawendi, V. Stevanović and T. Buonassisi, *Chem. Mater.*, 2017, **29**, 4667–4674.
24 Q. Lu, Y. Yu, Q. Ma, B. Chen and H. Zhang, *Adv. Mater.*, 2016, **28**, 1917–1933.
25 J. Chen, C. Dong, H. Idriss, O. F. Mohammed and O. M. Bakr, *Adv. Energy Mater.*,1902433. Q5
26 The conduction band edge of $CsPbBr_3$ nanocrystals (11 nm size) is −3.35 eV versus vacuum, see ref. 11.
27 G. F. Samu, R. A. Scheidt, P. V. Kamat and C. Janáky, *Chem. Mater.*, 2018, **30**, 561–569.
28 C. Liu, M. Hu, X. Zhou, J. Wu, L. Zhang, W. Kong, X. Li, X. Zhao, S. Dai, B. Xu and C. Cheng, *NPG Asia Mater.*, 2018, **10**, 552–561.
29 V. Stevanović, S. Lany, D. S. Ginley, W. Tumas and A. Zunger, *Phys. Chem. Chem. Phys.*, 2014, **16**, 3706–3714.
30 J. H. Rhee, C.-C. Chung and E. W.-G. Diau, *NPG Asia Mater.*, 2013, **5**, e68–e68.
31 Perovskite oxides have been used for microwave-induced catalytic oxidation of organic pollutants see ref. 32–35.
32 Y. Wang, Y. Wang, L. Yu, R. Wang and X. Zhang, *Chem. Eng. J.*, 2020, **390**, 124550.
33 Y. Wang, L. Yu, R. Wang, Y. Wang and X. Zhang, *J. Colloid Interface Sci.*, 2020, **564**, 392–405.
34 Y. Wang, Y. Wang, L. Yu, J. Wang, B. Du and X. Zhang, *Chem. Eng. J.*, 2019, **368**, 115–128.
35 Y. Wang, J. Wang, B. Du, Y. Wang, Y. Xiong, Y. Yang and X. Zhang, *Appl. Surf. Sci.*, 2018, **439**, 475–487.
36 M. Neumann, S. Füldner, B. König and K. Zeitler, *Angew. Chem., Int. Ed.*, 2011, **50**, 951–954.
37 M. Neumann, S. Füldner, B. König and K. Zeitler, *Angew. Chem.*, 2011, **123**, 981–985.
38 D. A. Koch, B. J. Henne and D. E. Bartak, *J. Electrochem. Soc.*, 1987, **134**, 3062–3067.
39 H.-W. Shih, M. N. Vander Wal, R. L. Grange and D. W. C. MacMillan, *J. Am. Chem. Soc.*, 2010, **132**, 13600–13603.
40 I. Rosa-Pardo, S. Pocoví-Martínez, R. Arenal, R. E. Galian and J. Pérez-Prieto, *Nanoscale*, 2019, **11**, 18065–18070.
41 V. K. Ravi, A. Swarnkar, R. Chakraborty and A. Nag, *Nanotechnology*, 2016, **27**, 325708.
42 A. Call, C. Casadevall, F. Acuña-Parés, A. Casitas and J. Lloret-Fillol, *Chem. Sci.*, 2017, **8**, 4739–4749.
43 L. Shi, C. He, D. Zhu, Q. He, Y. Li, Y. Chen, Y. Sun, Y. Fu, D. Wen, H. Cao and J. Cheng, *J. Mater. Chem.*, 2012, **22**, 11629–11635.
44 D. Cardenas-Morcoso, A. F. Gualdrón-Reyes, A. B. Ferreira Vitoreti, M. García-Tecedor, S. J. Yoon, M. Solis de la Fuente, I. Mora-Seró and S. Gimenez, *J. Phys. Chem. Lett.*, 2019, **10**, 630–636.
45 There are evidences of the occurance of halogen-exchange between $CsPbBr_3$ and alkane chlorides; this is consistent with interaction between the halides and the NC surface.
46 D. Parobek, Y. Dong, T. Qiao, D. Rossi and D. H. Son, *J. Am. Chem. Soc.*, 2017, **139**, 4358–4361.
47 W.-B. Wu, Y.-C. Wong, Z.-K. Tan and J. Wu, *Catal. Sci. Technol.*, 2018, **8**, 4257–4263.

